

A high order block finite difference, error inhibiting scheme for the transport equation

Adi Ditkowski, Anne Le Blanc, and Chi-Wang Shu

Abstract We propose a block finite difference, error inhibiting scheme that is fourth-order accurate for short to moderate times and has a six-order convergence rate for long times. This scheme outperforms the standard fourth-order Finite Difference scheme. We also demonstrate that the proposed scheme is a particular type of nodal-based Discontinuous Galerkin method with $p = 1$.

1 Introduction

The main theme of this manuscript is the construction and analysis of error-inhibiting block finite difference schemes for initial boundary value problems for PDEs. Applications to hyperbolic problems, namely the pure transport problem, are emphasized in this text.

Long-time numerical integration has become a significant issue in computational electrodynamics and fluid dynamics. A scheme might be stable in the classical sense (Lax stability), while its error grows exponentially in time [2]. Typically, the primary source of the error is the linearly growing phase error. The source of the phase error is that for each mode (frequency), the velocity of the numerical wave is slightly different from the analytical one. Therefore, reducing this phase error as much as possible is critical.

Adi Ditkowski
Tel Aviv University, Tel Aviv 69978, Israel e-mail: adid@tauex.tau.ac.il,

Anne Le Blanc
Tel Aviv University, Tel Aviv 69978, Israel, e-mail: anneleb@tauex.tau.ac.il

Chi-Wang Shu
Brown University, Providence, RI 02912, USA, e-mail: chi-wang_shu@brown.edu

The standard procedure to build Finite Difference (FD) schemes is first, constructing a *consistent* approximation for the given problem, and secondly, its *stability*, which is the discrete analog of well-posedness [3], is proven. Lax's equivalence theorem [4] ensures the convergence of the scheme, meaning that for a finite final time T , the numerical solution converges to the analytic solution of the problem as the mesh size goes to zero [5]. In the case of semi-discrete schemes, which is the class of schemes included in our work, stability is equivalent to the semi-boundedness of right hand side of the semi-discrete scheme. It implies that all eigenvalues of the coefficient matrix of the Ordinary Differential Equation (ODE) system have real parts bounded from above by a constant [3], as well as a full set of eigenvectors that remain independent as the mesh is refined. However, this analysis is not refined enough for our purpose.

We focus on the different aspects involved in constructing and analyzing an efficient numerical scheme called Block-Finite-Difference, derived from the classical FD method. The BFD schemes derived for the Heat equation (see [7], [14] for further details) relied on the inherent dissipation of the diffusion operator. This dissipation, as well as the post-processing procedure, caused the damping of the high-frequency elements of the error. The transport problem has no dissipation. Therefore, we rely on other mechanisms to manipulate the dynamics in which the error is accumulated in time.

The main idea behind the derivation of these BFD schemes for the transport problem is to manipulate the interaction between the truncation error and the dynamics of the scheme such that it inhibits the error from accumulating. In this manuscript, we derived a scheme with a third-order truncation error. However, the leading term of the error is of third-order, bounded in time, which can be eliminated in a post-processing stage to get fourth-order, bounded in time term, and the six-order phase error. Thus, this is a third-order or fourth-order after post-processing scheme for short to moderate times, while it is a six-order method for long times.

This manuscript is constructed as follows: in Section 2 we construct the block finite difference scheme, analyze its stability and accuracy, and present several numerical examples to demonstrate its properties. Section 3 shows that this scheme can be derived as a nodal-based DG method by adding extra penalty terms. Conclusions are given in Section 4

2 Block Finite Difference Methods for the Transport Problem

Consider the following problem

$$\begin{cases} \frac{\partial u}{\partial t} + \frac{\partial u}{\partial x} = 0, & x \in (0, 2\pi), \quad t \geq 0 \\ u(x, 0) = f(x) \end{cases} \quad (1)$$

with periodic boundary conditions.

We solve this problem over the following grid:

$$x_{j-1/4} = x_j - h/4, \quad x_{j+1/4} = x_j + h/4, \quad h = 2\pi/N, \quad j = 1, \dots, N \quad (2)$$

where

$$x_j = h(j-1) + \frac{h}{2} \quad (3)$$

Altogether there are $2N$ points on the grid, with a distance of $h/2$ between them.

Unlike the standard approach, we note here that the boundary points do not coincide with any grid nodes.

We consider the following approximation:

$$\mathbf{u}_x = \frac{1}{6h} \left[\begin{pmatrix} \ddots & \ddots & \ddots & \ddots & \ddots & \ddots & \ddots \\ & 1 & -8 & \mathbf{0} & 8 & -1 & \\ & & 1 & -8 & \mathbf{0} & 8 & -1 \\ & & & \ddots & \ddots & \ddots & \ddots \end{pmatrix} + c_1 \begin{pmatrix} \ddots & \ddots & \ddots & \ddots & \ddots & \ddots & \ddots \\ & 1 & -4 & \mathbf{6} & -4 & 1 & 0 \\ & & -1 & 4 & -6 & \mathbf{4} & -1 \\ & & & \ddots & \ddots & \ddots & \ddots \end{pmatrix} \right. \\ \left. + c_2 \begin{pmatrix} \ddots & \ddots & \ddots & \ddots & \ddots & \ddots & \ddots \\ & 0 & 1 & -\mathbf{4} & 6 & -4 & 1 \\ & & 0 & -1 & 4 & -\mathbf{6} & 4 \\ & & & \ddots & \ddots & \ddots & \ddots \end{pmatrix} \right] \mathbf{u} + \mathbf{T}_e = \mathbf{Q}\mathbf{u} + \mathbf{T}_e \quad (4)$$

The truncation error of this scheme is:

$$T_{e_{j-\frac{1}{4}}} = \frac{1}{11520} \left[120(c_1 + c_2)h^3 u^{(4)} + (-24 + 60c_2)h^4 u^{(5)} \right]_{x_{j-1/4}} + O(h^5) \quad (5)$$

$$T_{e_{j+\frac{1}{4}}} = \frac{1}{11520} \left[-120(c_1 + c_2)h^3 u^{(4)} + (-24 + 60c_1)h^4 u^{(5)} \right]_{x_{j+1/4}} + O(h^5)$$

Formally, this is a third-order scheme. Note, however, that the leading term is highly oscillatory.

2.1 Stability and Accuracy

Unlike the standard finite difference schemes, we need a more refined tool to analyze the BFD methods than estimating the truncation error and applying the Lax-Richtmyer equivalence theorem. Furthermore, since different stencils are used for the points $x_{j-\frac{1}{4}}$ and $x_{j+\frac{1}{4}}$, we cannot use the Fourier analysis directly. Therefore, we use the method proposed in [6], [7] and [14].

The analysis is based on the observation that if we split the Fourier spectrum into low and high frequencies as follows, let $\omega \in \{-N/2, \dots, N/2\}$ and:

$$\nu = \begin{cases} \omega - N, & \omega > 0 \\ \omega + N, & \omega \leq 0 \end{cases} \quad (6)$$

Then, for $\omega > 0$, we get the following relations:

$$e^{i\omega x_{j-1/4}} = ie^{i\nu x_{j-1/4}} \quad \text{and} \quad e^{i\omega x_{j+1/4}} = -ie^{i\nu x_{j+1/4}}. \quad (7)$$

Similarly, for $\omega \leq 0$, we obtain:

$$e^{i\omega x_{j-1/4}} = -ie^{i\nu x_{j-1/4}} \quad \text{and} \quad e^{i\omega x_{j+1/4}} = ie^{i\nu x_{j+1/4}}.$$

Let us assume first that $\omega > 0$. We denote the vectors $e^{i\omega \mathbf{x}}$ and $e^{i\nu \mathbf{x}}$ by:

$$e^{i\omega \mathbf{x}} = \begin{pmatrix} \vdots \\ e^{i\omega x_{j-1/4}} \\ e^{i\omega x_{j+1/4}} \\ \vdots \end{pmatrix}, \quad e^{i\nu \mathbf{x}} = \begin{pmatrix} \vdots \\ e^{i\nu x_{j-1/4}} \\ e^{i\nu x_{j+1/4}} \\ \vdots \end{pmatrix}$$

We look for eigenvectors in the form of:

$$\psi_k(\omega) = \alpha_k \frac{e^{i\omega \mathbf{x}}}{\sqrt{2\pi}} + \beta_k \frac{e^{i\nu \mathbf{x}}}{\sqrt{2\pi}} \quad (8)$$

where, for normalization, it is required that $|\alpha_k|^2 + |\beta_k|^2 = 1$, $k = 1, 2$. It follows that:

$$\begin{aligned} Qe^{i\omega \mathbf{x}} &= \text{diag}(\mu_1, \mu_2, \dots, \mu_1, \mu_2)e^{i\omega \mathbf{x}} \\ Qe^{i\nu \mathbf{x}} &= \text{diag}(\sigma_1, \sigma_2, \dots, \sigma_1, \sigma_2)e^{i\nu \mathbf{x}} \end{aligned} \quad (9)$$

where the matrix Q was defined in (4) and:

$$\begin{aligned} \mu_1 &= \frac{1}{3h} \left[-i \left(8 \sin \left(\frac{h\omega}{2} \right) - \sin(h\omega) \right) - 8 \sin^4 \left(\frac{h\omega}{4} \right) \left(c_1 + c_2 e^{\frac{ih\omega}{2}} \right) \right] \\ \mu_2 &= \frac{1}{3h} \left[-i \left(8 \sin \left(\frac{h\omega}{2} \right) - \sin(h\omega) \right) + 8 \sin^4 \left(\frac{h\omega}{4} \right) \left(c_1 e^{-\frac{ih\omega}{2}} + c_2 \right) \right] \\ \sigma_1 &= \frac{1}{3h} \left[i \left(8 \sin \left(\frac{h\omega}{2} \right) + \sin(h\omega) \right) - 8 \cos^4 \left(\frac{h\omega}{4} \right) \left(c_1 - c_2 e^{\frac{ih\omega}{2}} \right) \right] \\ \sigma_2 &= \frac{1}{3h} \left[i \left(8 \sin \left(\frac{h\omega}{2} \right) + \sin(h\omega) \right) - 8 \cos^4 \left(\frac{h\omega}{4} \right) \left(c_1 e^{-\frac{ih\omega}{2}} - c_2 \right) \right] \end{aligned}$$

We note here that this diagonal matrix is the same under the assumption that $\omega \leq 0$. In order to find the coefficients α_k, β_k and the eigenvalues (symbols) \hat{Q}_k for $\omega \neq 0$, we substitute ψ_k , defined at (8), into the equation $Q\psi_k = \hat{Q}_k\psi_k$ to get

$$\begin{aligned} \mu_1 \frac{\alpha_k}{\sqrt{2\pi}} e^{i\omega x_{j-\frac{1}{4}}} + \sigma_1 \frac{\beta_k}{\sqrt{2\pi}} e^{i\nu x_{j-\frac{1}{4}}} &= \hat{Q}_k \left(\frac{\alpha_k}{\sqrt{2\pi}} e^{i\omega x_{j-\frac{1}{4}}} + \frac{\beta_k}{\sqrt{2\pi}} e^{i\nu x_{j-\frac{1}{4}}} \right) \\ \mu_2 \frac{\alpha_k}{\sqrt{2\pi}} e^{i\omega x_{j+\frac{1}{4}}} + \sigma_2 \frac{\beta_k}{\sqrt{2\pi}} e^{i\nu x_{j+\frac{1}{4}}} &= \hat{Q}_k \left(\frac{\alpha_k}{\sqrt{2\pi}} e^{i\omega x_{j+\frac{1}{4}}} + \frac{\beta_k}{\sqrt{2\pi}} e^{i\nu x_{j+\frac{1}{4}}} \right) \end{aligned} \quad (10)$$

We can simplify (10), using the definition $r_k = i \frac{\beta_k}{\alpha_k}$ and obtain the system:

$$\begin{aligned} \mu_1 - \sigma_1 r_k &= \hat{Q}_k (1 - r_k) \\ \mu_2 + \sigma_2 r_k &= \hat{Q}_k (1 + r_k) \end{aligned} \quad (11)$$

The eigenvalues \hat{Q}_k , for all $\omega \neq 0$ are:

$$\begin{aligned} \hat{Q}_1(\omega) &= \frac{1}{12h} \left(\Omega - \sqrt{2\Delta} \right) \\ \hat{Q}_2(\omega) &= \frac{1}{12h} \left(\Omega + \sqrt{2\Delta} \right) \end{aligned} \quad (12)$$

where

$$\Omega = -4i(c_1 + c_2 + 1) \sin(\omega h) + 6(c_2 - c_1) \cos(\omega h) + 10(c_2 - c_1)$$

and

$$\begin{aligned} \Delta &= -80c_1 - 256 + 55c_1^2 + 55c_2^2 - 2(63c_1 + 40)c_2 + \\ &4 \left(15c_1^2 + c_1(16 - 30c_2) + c_2(15c_2 + 16) + 64 \right) \cos(\omega h) + \\ &\left(13c_1^2 + 2c_1(8 - 5c_2) + c_2(13c_2 + 16) \right) \cos(2\omega h) + \\ &8i(-c_1 + c_2) \sin(\omega h) \left((3c_1 + 3c_2 + 4) \cos(\omega h) + 5c_1 + 5c_2 + 28 \right) \end{aligned}$$

Using the normalization condition $|\alpha_k|^2 + |\beta_k|^2 = 1$, $k = 1, 2$, we choose the coefficients α_k and β_k to be:

$$\alpha_1 = \frac{1}{\sqrt{1 + |r_1|^2}}, \quad \beta_1 = -i \frac{r_1}{\sqrt{1 + |r_1|^2}} \quad (13)$$

$$\alpha_2 = i \frac{|r_2|/r_2}{\sqrt{1 + |r_2|^2}}, \quad \beta_2 = \frac{|r_2|}{\sqrt{1 + |r_2|^2}} \quad (14)$$

When $c_1 < c_2$, the real part of $\hat{Q}_1(\omega)$ is strictly positive. Therefore, the scheme is unstable; hence, we will consider the cases where $c_1 \geq c_2$.

2.1.1 Stability proof using eigenvalues and eigenvectors properties

For any $c_1 \geq c_2$, it was numerically shown that the real part of the eigenvalues $\hat{Q}_1(\omega), \hat{Q}_2(\omega)$ is non-positive. Therefore, the scheme is Von-Neumann stable. We next prove that the operator Q has a full set of eigenvectors for any ωh .

In the case where $\omega = 0$, the corresponding eigenvectors are $\psi_1(0) = e^{i0\mathbf{x}}, \psi_2(0) = e^{i(N+1)\mathbf{x}}$ and their corresponding eigenvalues $\hat{Q}_1(0) = 0, \hat{Q}_2(0) = (8(-c_1 + c_2))/(3h)$;

Otherwise, by construction, $\psi_k(\omega_1)$ and $\psi_l(\omega_2)$, $k, l = 1, 2$ are orthogonal, for any $\omega_1 \neq \omega_2$.

Unlike the Fourier mode $e^{i\omega\mathbf{x}}, \psi_k(\omega)$ are not orthogonal, since $\langle \psi_1(\omega), \psi_2(\omega) \rangle_h = \sum_j \frac{h}{2} \overline{\psi_1(\omega)_j} \psi_2(\omega)_j \neq 0$ where the inner product $\langle \cdot, \cdot \rangle_h$ is the scalar inner product normalized by $h/2$.

Let us define the cosine of the angle $\theta(\omega)$ between the complex vectors $\psi_1(\omega)$ and $\psi_2(\omega)$ as follows :

$$\cos(\theta(\omega)) = \frac{|\langle \psi_1(\omega), \psi_2(\omega) \rangle_h|}{\|\psi_1(\omega)\| \|\psi_2(\omega)\|}$$

In fact, we can compute $\cos(\theta(\omega))$ between the vectors using the definition of r_1 and r_2 , the normalization condition on α_k, β_k and (7).

It yields

$$\cos(\theta(\omega)) = \left| \overline{\alpha_1} \alpha_2 + \overline{\beta_1} \beta_2 \right| = \frac{1}{\sqrt{1 + |r_1|^2}} \frac{|r_2|}{\sqrt{1 + |r_2|^2}} \left| \frac{1}{r_2} + r_1 \right|$$

It can be shown that $|\cos(\theta(\omega))| < 0.4$ for any value $-1 \leq c_2 \leq c_1 \leq 1$ and all $-\pi \leq \omega h \leq \pi$. Therefore, we conclude that the scheme is stable for these values of c_1 and c_2 .

In the next part of the section, we proceed with the asymptotic analysis of the eigenvalues. For the accuracy analysis, it is sufficient to demonstrate the behaviour of the approximate solution for $\omega h \ll 1$, since, for a solution u which lays in C^p , its Fourier coefficient $\hat{u}(\omega)$ decays as $const/|\omega|^{p+1}$.

2.2 The $c_1 > c_2$ case

For $\omega h \ll 1$, the eigenvalues $\hat{Q}_k(\omega)$, see (12), are:

$$\hat{Q}_1(\omega) = -i\omega + \frac{1}{480} i h^4 \omega^5 - \frac{h^5 \omega^6 (c_1 + c_2)}{384(c_1 - c_2)} + O(h^6)$$

and

$$\begin{aligned}\hat{Q}_2(\omega) = & -\frac{8(c_1-c_2)}{3h} + \frac{1}{3}i\omega(2c_1+2c_2+5) + \frac{1}{2}h\omega^2(c_1-c_2) - \frac{1}{9}ih^2\omega^3(c_1+c_2+1) + \\ & \frac{1}{24}h^3\omega^4(c_2-c_1) + O(h^4)\end{aligned}$$

The different values for $\alpha_1, \alpha_2, \beta_1$ and β_2 are

$$\begin{aligned}\alpha_1 = & 1 - \frac{(h\omega)^8(c_1+c_2)^2}{131072(c_1-c_2)^2} + O(h^9) \\ \beta_1 = & -\frac{i(h\omega)^4(c_1+c_2)}{256(c_1-c_2)} + \frac{(h\omega)^5(c_1c_2+c_1+c_2)}{256(c_1-c_2)^2} + O(h^6) \\ \alpha_2 = & \frac{h\omega}{4} + \frac{i(h\omega)^2}{4c_1-4c_2} - \frac{(h\omega)^3(c_1^2-2c_1(c_2-12)+c_2(c_2+24)+96)}{384(c_1-c_2)^2} + O(h^4) \\ \beta_2 = & 1 - \frac{1}{32}(h\omega)^2 + \frac{(h\omega)^4(-2c_1c_2+c_1(c_1+96)+c_2^2+96(c_2+2))}{6144(c_1-c_2)^2} + O(h^6)\end{aligned}$$

We note here that it is assumed that the initial data lies only in the low frequencies.

Assuming the initial condition $u(x, 0) = e^{i\omega x}$, or

$$v_{j-1/4}(0) = e^{i\omega x_{j-1/4}}, v_{j+1/4}(0) = e^{i\omega x_{j+1/4}}; \quad h\omega \ll 1$$

we obtain, using the expansions for $\hat{Q}_k(\omega)$, $\alpha_1, \alpha_2, \beta_1$ and β_2 , the expression of the scheme exact solution at $x_{j-1/4}$.

$$\begin{aligned}v_{j-\frac{1}{4}}(t) = & \left(e^{-i\omega t} \left[1 + \frac{i\omega^5 t h^4}{480} - \frac{(\omega h)^5(c_1+c_2)(8t\omega+3i)}{3072(c_1-c_2)} \right] + O(h^6) \right) e^{i\omega x_{j-\frac{1}{4}}} + \\ & e^{-i\omega t} \left(\frac{(\omega h)^5(c_1c_2+c_1+c_2)}{256(c_1-c_2)^2} - \frac{i(\omega h)^4(c_1+c_2)}{256(c_1-c_2)} + O(h^6) \right) e^{i\omega x_{j-\frac{1}{4}}} \quad (15)\end{aligned}$$

A similar expression holds for $x_{j+1/4}$. Therefore, the scheme has a fourth-order convergence rate, for all $c_1 > c_2$.

We note here that the order of magnitude of α_1 and β_2 is 1, whereas β_1 is of order h^4 and α_2 is of order h . Hence, since the exact solution is $e^{-i\omega t}$, the exact solution of the equation is well approximated by the low frequencies represented by ω , while the truncation error lies with the high frequencies ν .

2.3 The $c_1 = c_2$ case

We now explore the case $c_1 = c_2 = c$. In this case, the $\hat{Q}_k(\omega)$ become:

$$\hat{Q}_1(\omega) = \frac{1}{3h} \left(-2\sqrt{2} \sin\left(\frac{h\omega}{2}\right) \sqrt{-(c+2)(c \cos(h\omega) + c + 4)} + i(2c+1) \sin(h\omega) \right)$$

$$\hat{Q}_2(\omega) = \frac{1}{3h} \left(2\sqrt{2} \sin\left(\frac{h\omega}{2}\right) \sqrt{-(c+2)(c \cos(h\omega) + c + 4)} + i(2c+1) \sin(h\omega) \right)$$

Following the same procedure as in the previous section, we conclude that for $\omega h \ll 1$, the eigenvalues are:

$$\hat{Q}_1(\omega) = -i\omega + \frac{i(1-2c)h^4\omega^5}{240(c+2)} + O(h^6)$$

and

$$\hat{Q}_2(\omega) = \frac{1}{3}i(4c+5)\omega - \frac{1}{9}i(2c+1)h^2\omega^3 + \frac{i(8c^2+26c+5)h^4\omega^5}{720(c+2)} + O(h^6)$$

$\alpha_1, \alpha_2, \beta_1$ and β_2 are:

$$\alpha_1 = 1 - \frac{c^2\omega^6h^6}{8192(c+2)^2} + O(h^{10}), \quad \beta_1 = \frac{c\omega^3h^3}{64(c+2)} + \frac{c(c-2)\omega^5h^5}{1024(c+2)^2} + O(h^7)$$

and

$$\alpha_2 = \frac{c\omega h}{4c+8} - \frac{c(c^2+16c+40)\omega^3h^3}{384(c+2)^3} + O(h^5), \quad \beta_2 = 1 - \frac{c^2\omega^2h^2}{32(c+2)^2} + O(h^4)$$

Assuming the initial condition $u(x, 0) = e^{i\omega x}$, or

$$v_{j-1/4}(0) = e^{i\omega x_{j-1/4}}, v_{j+1/4}(0) = e^{i\omega x_{j+1/4}}; \quad \omega h \ll 1$$

and we obtain, for $\omega > 0$, the expression of the scheme exact solution at $x_{j-1/4}$.

$$\begin{aligned} v_{j-\frac{1}{4}}(t) &= \left[e^{-i\omega t} e^{i \left(\frac{(1-2c)\omega^5h^4}{240(c+2)} - \frac{(2c^2-6c+1)\omega^7h^6}{4032(c+2)^2} + O(\omega^9h^8) \right) t} \right] e^{i\omega x_{j-\frac{1}{4}}} + \\ &\quad \left[\left(\frac{c^2\omega^4h^4}{256(c+2)^2} + O(\omega^6h^6) \right) \times \left(e^{-i(\omega+O(\omega^5h^4))t} - e^{i(\frac{1}{3}(4c+5)\omega+O(\omega^3h^2))t} \right) \right] e^{i\omega x_{j-\frac{1}{4}}} + \\ &\quad \left[\left(\frac{c\omega^3h^3}{64(c+2)} + O(\omega^5h^5) \right) \times \left(e^{-i(\omega+O(\omega^5h^4))t} - e^{i(\frac{1}{3}(4c+5)\omega+O(\omega^3h^2))t} \right) \right] e^{i\omega x_{j-\frac{1}{4}}} \end{aligned} \quad (16)$$

Similar expressions holds for $x_{j+1/4}$ and $\omega \leq 0$. There are three sources for the error. The third one is a third-order, bounded in time high-frequency term. This term, however, can be eliminated in a post-processing stage. The second one is a fourth-order, low-frequency one. This term is also bound in time. The first term is a

phase error. It grows linearly in time, at least until the error is approximately in order of 1. The phase error is fourth-order; however, it can be made six-order by taking $c = 1/2$.

Therefore, for the $c = 1/2$ case, what we expect to see for short to moderate times is a third-order error, bounded in time, which can be filtered using a post-processing filter to get a bounded-in-time fourth-order error. When the six-order linearly growing phase error becomes dominant, this scheme behaves like a standard six-order finite difference scheme. It should be noted that the error in the standard finite difference scheme is a linearly growing phase error.

We demonstrate this behavior in the next section.

2.4 Numerical examples

In this section, we illustrate the properties of the BFS method presented in the previous section using a few numerical examples.

$$\begin{cases} \frac{\partial u}{\partial t} + \frac{\partial u}{\partial x} = 0, & x \in (0, 2\pi), t \geq 0 \\ u(x, 0) = \exp \cos(2\pi(x)) \end{cases} \quad (17)$$

The exact solution to this problem is $u(x, t) = \exp \cos(2\pi(x-t))$. Scheme (4) was run, for different values of c_1, c_2 , on the interval $[0, 1]$ with $N = 48, 60, 72, 96, 120, 144$, and the final time was $T = 1$. A six-order explicit Runge-Kutta method was used for time propagation. The convergence plots are presented in Fig. 1.

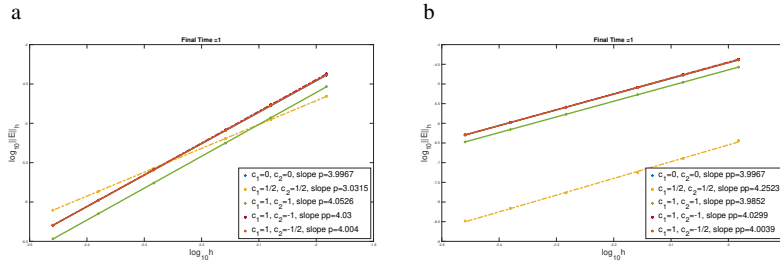


Fig. 1 Scheme (4) Convergence plots, $\log_{10} \|E\|$ vs. $\log_{10} h$, for different values of c_1, c_2 . Final time, $T = 1$ -a: no post-processing; b: spectral post-processing

As shown in Fig. 1a, where $c_1 = -c_2$, the truncation error, (5), and the scheme are fourth-order. In the case $c_1 = 1$ and $c_2 = -1/2$, where $c_1 > c_2$, it is a fourth-order scheme, although the truncation error is only third-order. When $c_1 = c_2 = 1/2$, the scheme is indeed third-order; however, when $c_1 = c_2 = 1$, the convergence rate is

four due to the cancellation of the leading terms of the bounded parts of the error at integer times, see equation (16). After post-processing, see Fig. 1b, the scheme has a fourth-order convergence rate. The error for the $c_1 = c_2 = 1/2$ case is two orders of magnitude smaller since it is caused only by the bounded part of the error, and the linearly growing, six-order phase error is neglectable.

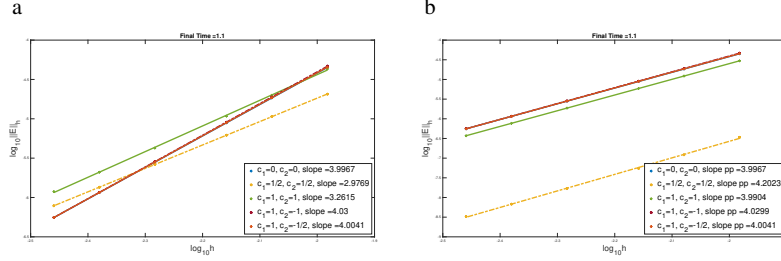


Fig. 2 Scheme (4) Convergence plots, $\log_{10} \|E\|$ vs. $\log_{10} h$, for different values of c_1, c_2 . Final time, $T = 1.1$ -a: no post-processing; b: spectral post-processing

When the final time is $T = 1.1$, see Fig. 2, the scheme has a third-order convergence rate for $c_1 = c_2 = 1$, which can be filtered to be fourth-order after the post-processing. Since the phase error is of fourth order, the error is comparable to the other $c_1 > c_2$ cases.

To examine the long-time behavior of the scheme for $c_1 = c_2$, we ran the example for $T = 100$ and $T = 1000$: the analysis, eq. (16) shows that for $c_1 = c_2 = 1/2$, the scheme convergence rate becomes six-order when the phase error becomes dominant. The convergence rates presented in Fig. 3 demonstrate this phenomenon.

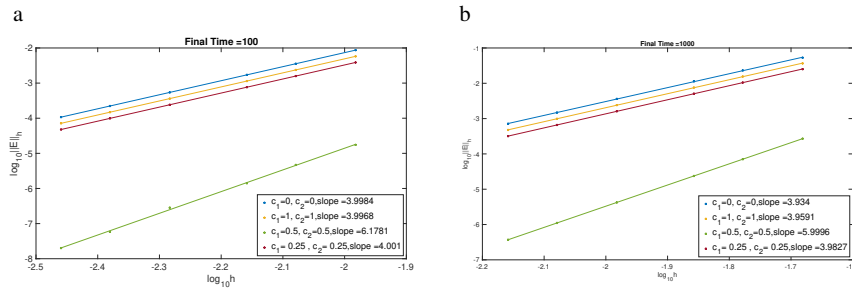


Fig. 3 Scheme (4), Convergence plots, $\log_{10} \|E\|$ vs. $\log_{10} h$ - Periodic BC for $c_1 = c_2$, with post processing, for different final times. a: $T = 100$, b: $T = 1000$.

To illustrate the effect of the phase error for long-time propagations, we ran the scheme with the initial condition $f(x) = \sin(4\pi(x))$ with $N = 32$ (64 degrees of

freedom) to $T = 4800$. We compare the cases $c_1 = c_2 = 0$, the standard fourth-order FD scheme, and $c_1 = c_2 = 1/2$, with and without post-processing. The results are shown in Fig. 4. While the standard scheme has a 180° phase error, the $c_1 = c_2 = 1/2$, solution is undistinguished from the exact solution, at least in the eyeball norm. This observation is valid for both the un-post-processed and the post-processed cases.

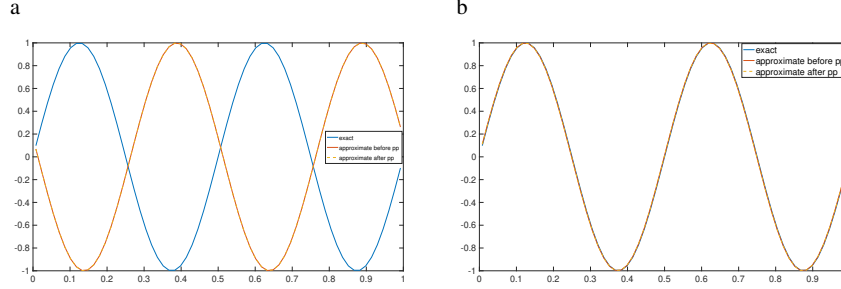


Fig. 4 The exact numerical solutions for $u(x, t) = \sin(4\pi(x - t))$, final time $T = 4800$ and $N = 32$ with post processing. a: standard fourth-order scheme, $c_1 = c_2 = 0$, b: $c_1 = c_2 = 1/2$.

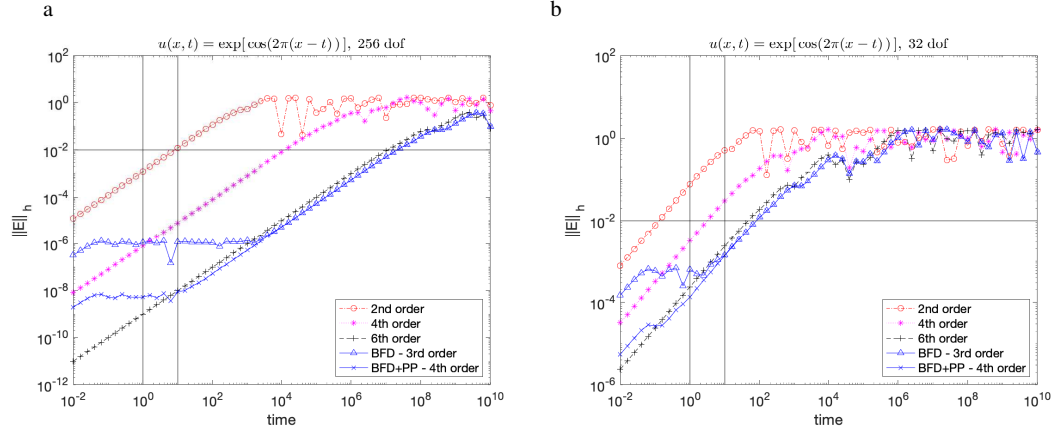


Fig. 5 The evolution of the error in time for the standard second, fourth, and six-order finite difference schemes and the BFD scheme, (4), with $c_1 = c_2 = 1/2$ with and without post-processing. a: for $N = 128$ (256 degrees of freedom), b: for $N = 16$ (32 degrees of freedom).

To examine the way the errors evolved in time, we solved the problem (17) to $T = 10^{10}$ using the standard second, fourth, and six-order finite difference schemes and the BFD scheme, (4), with $c_1 = c_2 = 1/2$ with and without post-processing.

We computed the time propagation by calculating the matrix $\exp(Qt)$. For the standard schemes, the errors grow linearly in time, as they are phase errors. For the $c_1 = c_2 = 1/2$ case, the third-order error and fourth-order after post-processing are bounded in time. When the six-order linearly growing phase error becomes dominant, this scheme behaves like a standard six-order finite difference scheme. The magnitudes of the errors and the rate at which the phase errors grow in time depend on N (or h). Thus, for high resolution, $N = 128$ (256 degrees of freedom), the phase error becomes dominant at $t \approx 10$ for the post-processed solution and at $t \approx 1000$ for the unprocessed one. Thus, for low resolution, $N = 16$ (32 degrees of freedom), the phase error becomes dominant at $t \approx 1$ for the unprocessed solution and almost immediately for the processed one, as illustrated in Fig. 5.

3 Equivalence to DG Method

This section shows that Scheme (4) is also a nodal-based, $p = 1$, Discontinuous Galerkin (DG) scheme. This DG scheme has a fourth-order (after post-processing) order of convergence for short times and six-order for long times, whereas the standard DG scheme with $p = 1$ is typically a second-order method.

3.1 Standard DG scheme

Discontinuous Galerkin (DG) methods are a particular class of finite element methods using discontinuous basis functions. We start by deriving a standard DG method as illustrated in [11] and [12].

Consider the transport equation (1), with periodic boundary conditions.

$$\begin{cases} \frac{\partial u}{\partial t} + \frac{\partial u}{\partial x} = 0, & x \in (0, 2\pi), \quad t \geq 0 \\ u(x, 0) = f(x) \end{cases} \quad (18)$$

We assume the following mesh to cover the computational domain $[0, 2\pi]$, consisting of cells

$$I_j = [x_{j-1/2}, x_{j+1/2}] \quad , \quad j = 1, \dots, N$$

where

$$0 = x_{1/2} < x_{3/2} < \dots < x_{N+1/2} = 2\pi$$

The center of each cell is located at $x_j = \frac{1}{2} (x_{j-1/2} + x_{j+1/2})$ and the size of each cell is $\Delta x_j = x_{j+1/2} - x_{j-1/2}$. We consider a uniform mesh, hence $h = \Delta x = \frac{2\pi}{N}$.

The discontinuous Galerkin scheme is defined as follows: Find $u, v \in V_{\Delta x}$ (where $V_{\Delta x} = \{v : v \text{ is a polynomial of degree at most } p \text{ for } x \in I_j, j = 1, \dots, N\}$) such that:

$$\int_{I_j} u_t v dx - \int_{I_j} u v_x dx + \hat{u}_{j+\frac{1}{2}} v_{j+1/2}^- - \hat{u}_{j-\frac{1}{2}} v_{j-1/2}^+ = 0 \quad (19)$$

for all $v \in V_{\Delta x}$. In our case, the information flows from left to right; we chose the upwind flux:

$$\begin{aligned} \hat{u}_{j+\frac{1}{2}} &= u_{j+\frac{1}{2}}^- \\ \hat{u}_{j-\frac{1}{2}} &= u_{j-\frac{1}{2}}^- \end{aligned} \quad (20)$$

Where a linear element basis, $p = 1$, is used on an equidistant grid, $x_{j-1/4}$ and $x_{j+1/4}$, $u(x)$ and $v(x)$ have the form

$$\begin{aligned} u(x) &= u_{j-1/4} \varphi_{j-1/4} + u_{j+1/4} \varphi_{j+1/4} \\ v(x) &= v_{j-1/4} \varphi_{j-1/4} + v_{j+1/4} \varphi_{j+1/4} \end{aligned} \quad (21)$$

where the Lagrange interpolating polynomials $\varphi_{j\pm 1/4}$ are

$$\begin{aligned} \varphi_{j-1/4} &= -\frac{2}{\Delta x} (x - x_{j+\frac{1}{4}}) \\ \varphi_{j+1/4} &= \frac{2}{\Delta x} (x - x_{j-\frac{1}{4}}) \end{aligned} \quad (22)$$

Collecting the coefficients of $v_{j-1/4}$ and $v_{j+1/4}$ yields the equation for the time derivative of $u_{j-1/4}$ and $u_{j+1/4}$

$$\begin{bmatrix} u_{j-1/4} \\ u_{j+1/4} \end{bmatrix}_t = \left(A \begin{bmatrix} u_{j-5/4} \\ u_{j-3/4} \end{bmatrix} + B \begin{bmatrix} u_{j-1/4} \\ u_{j+1/4} \end{bmatrix} + C \begin{bmatrix} u_{j+3/4} \\ u_{j+5/4} \end{bmatrix} \right) \quad (23)$$

where

$$A = \frac{1}{4h} \begin{bmatrix} -5 & 15 \\ 1 & -3 \end{bmatrix}, \quad B = \frac{1}{4h} \begin{bmatrix} -7 & -3 \\ 11 & -9 \end{bmatrix}, \quad C = \frac{1}{4h} \begin{bmatrix} 0 & 0 \\ 0 & 0 \end{bmatrix} \quad (24)$$

We note here that the standard DG scheme has a second order accuracy ($k + 1$ order, where $k = 1$ in our example).

3.2 Proof of equivalence

We can write Scheme (4) in the same form as (23), by assembling the matrices A , B and C are defined as follows:

$$\begin{aligned} A &= \frac{1}{6h} \begin{bmatrix} -1 - c_1 & 8 + 4c_1 - c_2 \\ c_1 & -1 - 4c_1 + c_2 \end{bmatrix}, \quad B = \frac{1}{6h} \begin{bmatrix} -6c_1 + 4c_2 & -8 + 4c_1 - 6c_2 \\ 8 + 6c_1 - 4c_2 & -4c_1 + 6c_2 \end{bmatrix} \\ C &= \frac{1}{6h} \begin{bmatrix} 1 - c_1 + 4c_2 & -c_2 \\ -8 + c_1 - 4c_2 & 1 + c_2 \end{bmatrix} \end{aligned} \quad (25)$$

Hence, our goal is to find the corresponding weak formulation of the problem numerical fluxes and possibly other penalty terms, such that the BFD scheme can be viewed as a form of DG scheme.

As done in Section 3.1, we choose a linear element basis (21) for the test and trial functions.

After replacing boundary terms with fluxes and the test function by its values inside the cell, the scheme becomes:

$$\int_{I_j} u_t v dx - \int_{I_j} u v_x dx + \hat{u}_{j+1/2} v_{j+1/2}^- - \hat{u}_{j-1/2} v_{j-1/2}^+ = 0 \quad (26)$$

By using the upwind flux and adding in Eq.(26) and adding all the possible penalty terms with general coefficients, we obtain the following scheme:

$$\begin{aligned} \int_{x_{j-1/2}}^{x_{j+1/2}} u_t v dx - \int_{I_j} u v_x dx &= \int_{x_{j-1/2}}^{x_{j+1/2}} u v_x dx - \hat{u}_{j+1/2} v_{j+1/2}^- + \hat{u}_{j-1/2} v_{j-1/2}^+ + \\ &\left(C_1 \left((u)_{j+1/2}^+ - (u)_{j+1/2}^- \right) + h C_2 \left((u_x)_{j+1/2}^+ - (u_x)_{j+1/2}^- \right) \right) v_{j+1/2}^- - \\ &\left(D_1 \left((u)_{j-1/2}^+ - (u)_{j-1/2}^- \right) + h D_2 \left((u_x)_{j-1/2}^+ - (u_x)_{j-1/2}^- \right) \right) v_{j-1/2}^+ + \\ &\left(h E_1 \left((u)_{j+1/2}^+ - (u)_{j+1/2}^- \right) + h^2 E_2 \left((u_x)_{j+1/2}^+ - (u_x)_{j+1/2}^- \right) \right) (v_x)_{j+1/2}^- - \\ &\left(h F_1 \left((u)_{j-1/2}^+ - (u)_{j-1/2}^- \right) + h^2 F_2 \left((u_x)_{j-1/2}^+ - (u_x)_{j-1/2}^- \right) \right) (v_x)_{j-1/2}^+ \end{aligned} \quad (27)$$

where, as stated above, the following upwind flux was chosen:

$$\hat{u}_{j+1/2} = u_{j+1/2}^-, \quad \hat{u}_{j-1/2} = u_{j-1/2}^- \quad (28)$$

The design of the above scheme is based on the minimal requirement that if $(u)_{j\pm 1/2}^+ = (u)_{j\pm 1/2}^-$ and $(u_x)_{j\pm 1/2}^+ = (u_x)_{j\pm 1/2}^-$, all penalties vanish.

We now write u and v in terms of their nodal values, then replacing $v(x)$ by $\varphi_{j+1/4}$ and then $\varphi_{j-1/4}$ and comparing with Eq.(27), to obtain a system of eight equations for eight unknowns. The unique solution to these equations is:

$$\begin{aligned} C_1 = D_1 &= -\frac{1}{2}, & C_2 = D_2 &= -\frac{1}{12}, & E_2 = F_2 &= \frac{1}{72}(c_1 - c_2) \\ E_1 &= \frac{1}{36}(2c_1 - 6c_2 + 1), & F_1 &= \frac{1}{36}(-6c_1 + 2c_2 + 1) \end{aligned}$$

This completes the proof that the BFD scheme (4) can be viewed as a particular type of $p = 1$, nodal-based DG scheme.

4 Conclusions

The BFD schemes derived for the Heat equation (see [7], [14] for further details) relied on the inherent dissipation of the diffusion operator. This dissipation, as well as the post-processing procedure, caused the damping of the high-frequency elements of the error. For the Transport problem, we had to rely on other mechanisms to manipulate the errors. For the correct choice of parameters, $c_1 = c_2 = 1/2$, we could have a third-order term, bounded in time, that can be eliminated in a post-processing stage, a fourth-order, bounded in time term, and the six-order phase error. Thus, this is a third-order or fourth-order after post-processing scheme for short to moderate times, while it is a six-order method for long times. Note that the truncation error is only of third order.

We also demonstrated that the BFD scheme is a particular type of nodal-based, $p = 1$, DG scheme.

An immediate extension of the current work is to adapt the proposed methodology to non-periodic boundary conditions, such as Dirichlet conditions, as was done in [10], for the Heat equation by creating ghost points outside the computational domain and extrapolating. Another extension would be to adapt the scheme to higher dimensions, such as 2D and 3D. The generalization to two dimensions is fairly straightforward, as the two-dimensional scheme is constructed as a tensor product of the one-dimensional scheme. This work may lead the way for constructing highly efficient DG methods.

5 Acknowledgement

This research was supported by Binational (US-Israel) Science Foundation grant No. 2016197.

References

1. Ditkowski, A.: Bounded-Error Finite Difference Schemes for Initial Boundary Value Problems on Complex Domains (PhD Thesis).
2. Carpenter, M. H., Gottlieb, D., Abarbanel, S.: Time-stable boundary conditions for finite-difference schemes solving hyperbolic systems: Methodology and application to high-order compact schemes. *J. Comput. Phys.* **111**, 220-236 (1994)
3. Gustafsson, B., Kreiss, H.-O., Oliger, J.: Time dependent problems and difference methods. John Wiley & Sons, New York (1995)
4. Lax, Peter D., Richtmyer, Robert D.: Survey of the stability of linear finite difference equations. *Communications on pure and applied mathematics* **9**, 267-293 (1956)
5. Richtmyer, R. D., Morton, K. W.: Difference Methods for Initial-Value Problems. Interscience Publishers, New York (1967)

6. Ditkowski, A.: High order finite difference schemes for the heat equation whose convergence rates are higher than their truncation errors. In: Spectral and High Order Methods for Partial Differential Equations ICOSAHOM 2014, pp. 167-178. Springer, New York (2015)
7. Ditkowski, A., Fink Shustin, P.: Error Inhibiting Schemes for Initial Boundary Value Heat Equation.
<https://arxiv.org/abs/2010.00476>. Cited 2020
8. Ditkowski, A., Gottlieb, S., Grant, Z.J.: Explicit and implicit error inhibiting schemes with post-processing. *Computers & Fluids* **208**, 104534 (1956)
9. Ditkowski, A., Gottlieb, S., Grant, Z.J.: Explicit and implicit error inhibiting schemes with post-processing. *SIAM Journal on Numerical Analysis* **58**, 3197–3225 (2020)
10. Le Blanc, A.: Error Inhibiting Methods for Finite Elements (PhD Thesis).
<https://anneleblanc08.wixsite.com/anneleblancmath>
11. Zhang, M., Shu, C.-W.: An analysis of three different formulations of the discontinuous Galerkin method for diffusion equations. *Mathematical Models and Methods in Applied Sciences* **13**, 395-413 (2003)
12. Cockburn, B.: Discontinuous Galerkin methods. *ZAMM - Journal of Applied Mathematics and Mechanics / Zeitschrift für Angewandte Mathematik und Mechanik* **83**, 731-754 (2003)
13. Guo, W., Zhong, X., Qiu, J.-M.: Superconvergence of discontinuous Galerkin and local discontinuous Galerkin methods: Eigen-structure analysis based on Fourier approach. *J. Comput. Phys.* **235**, 458-485 (2020)
14. Ditkowski, A., Le Blanc, A., Shu, C.-W.: Error Inhibiting Methods for Finite Elements.
<https://arxiv.org/abs/2010.00476>. Cited 2020